GA–A26732

DEUTERIUM VELOCITY AND TEMPERATURE MEASUREMENTS ON THE DIII-D TOKAMAK

by
B.A. GRIERSON, K.H. BURRELL, W.A. SOLOMON
and N.A. PABLANT

JUNE 2010

GENERAL ATOMICS

DISCLAIMER

GA–A26732

DEUTERIUM VELOCITY AND TEMPERATURE MEASUREMENTS ON THE DIII-D TOKAMAK

by
B.A. GRIERSON,* K.H. BURRELL, W.A. SOLOMON*
and N.A. PABLANT†

This is a preprint of a paper to be presented at the 18th Topical Conference on High Temperature Plasma Diagnostics, May 16–20, 2010 in Wildwood, New Jersey and to be published in Review of Scientific Instruments.

*Princeton Plasma Physics Laboratory, Princeton, New Jersey
†University of California-San Diego, La Jolla, California

Work supported in part by
the U.S. Department of Energy
under DE-AC02-09CH11466, DE-FC02-04ER54698
and DE-FG02-07ER54917

GENERAL ATOMICS ATOMICS PROJECT 30200
JUNE 2010

ABSTRACT

Newly installed diagnostic capabilities on the DIII-D tokamak [J.L. Luxon, Nucl. Fusion **46**, 6114 (2002)] enable the measurement of main ion (deuterium) velocity and temperature by charge exchange recombination (CER) spectroscopy. The uncertainty in atomic physics corrections for determining the velocity are overcome by exploiting the geometrical dependence of the apparent velocity on the viewing angle with respect to the neutral beam.

I. INTRODUCTION

Charge exchange spectroscopy of light impurities is the standard technique for determining ion temperature, plasma velocity and impurity concentration in tokamaks.[1–3] Measurement of the ion temperature and velocity is typically done for impurities in deuterium fueled devices because of the complexity of the spectrum near the D_α wavelength. Efforts have been made to spectroscopically measure the deuterium ion temperature in TEXTOR[4] as well as temperature and density on JET,[5,6] but spectroscopy of the main ion temperature and rotation has not been made standard practice on any machine. However, measurement of the properties of the main ion species is of primary importance in fusion scale tokamaks to assess the performance of such devices. The difference between the rotation velocity of impurity species and the main ions has consequences when comparing the theoretical critical MHD stability rotation velocity of the main ions with measurements based on impurities.[7] In cases of low rotation (such as with balanced neutral beam torque) or in future devices with low net momentum input (such as ITER), the impurity and main ion velocities can even have the opposite sign. The difference in toroidal rotation of the main ion and impurities depends on their respective pressure gradients and poloidal flows.[8,9] The predictions of this differential rotation are based on neoclassical theory, and remain to be validated. The intrinsic rotation[10] velocity, which is the toroidal rotation observed with zero net torque input, has yet to be investigated experimentally with direct measurement of the main ion rotation across the plasma radius in deuterium plasmas. When the collision frequency between main ions and impurity species is high enough, the temperatures are equilibrated; however, in low densities when the collisional coupling is weak, the temperatures can diverge. Plasma heating by neutral beams preferentially heats fully ionized impurities because of the Z_i dependence of the Coulomb collision, and can result in a higher inferred temperature when impurities are used.[11–13] Charge exchange velocity measurements are complicated by the energy dependence of the charge exchange cross-section.[14,15] The energy dependence of the charge exchange cross section produces distortions to the observed spectrum, resulting in an apparent shift in the spectrum that is not associated with Doppler motion. The resulting apparent velocity can differ from the true velocity by more than 100 km/s in high temperature discharges. The apparent velocity is typically corrected to recover the true plasma velocity using atomic physics calculations.[15] By utilizing views of both co and counter (with respect to plasma current) beams, the effects of uncertainties in the atomic calculations on the velocity measurement can be overcome.

II. EXPERIMENTAL CONFIGURATION

A prototype two-chord diagnostic for the measurement of deuterium ion temperature and toroidal velocity viewing deuterium neutral beam injection is operational as an addition to the DIII-D CER system.[16,17] The diagnostic views beams which inject both in the co-current and counter-current direction. The unique viewing configuration of co and counter beams permits a direct measurement of the toroidal rotation without relying on atomic physics cross-sections.[18] The measured apparent velocity is given by $\mathbf{V}_{app} = \mathbf{V}_{true} + \alpha \hat{\mathbf{V}}_b$, where $\mathbf{V}_{true}$ is the true rotation velocity, α is a scalar quantity containing the atomic physics, and $\hat{\mathbf{V}}_b$ is the unit vector along the neutral beam. The true velocity $\mathbf{V}_{true}$ is a combination of direct charge exchange and halo emission (described in section III). With independent views of the co and counter beam at the same major radius, the true velocity and associated correction can be calculated. Each neutral beam has two ion sources directed at different angles, identified by 'RT' and 'LT' for right or left ion source. The two main ion viewing chords intersect the 30°RT and 210°LT neutral beams at nearly identical major radii 172.86 cm, 173.26 cm and angles from the neutral beam injection direction of 55:72°, 103:55° respectively (Fig. 1).

The light from the tokamak is collected and focused by a f/4 lens, transmitted through 1500 μm fiber to a SPEX 3/4 m spectrometer. The dispersed light is then collected by a charge coupled device (CCD) camera with 1024 pixel width. The spectrometer has a dispersion of 0.170Å/pixel in first order. A wavelength calibration is performed after each tokamak discharge by using light from a neon calibration lamp. Three neon lines are used for shot-to-shot calibration of dispersion and wavelength fiducial. White light exposure provides the intensity response to a broadband light source and is compensated for in the spectral analysis. Spectra are obtained at 2.5 ms integration time.

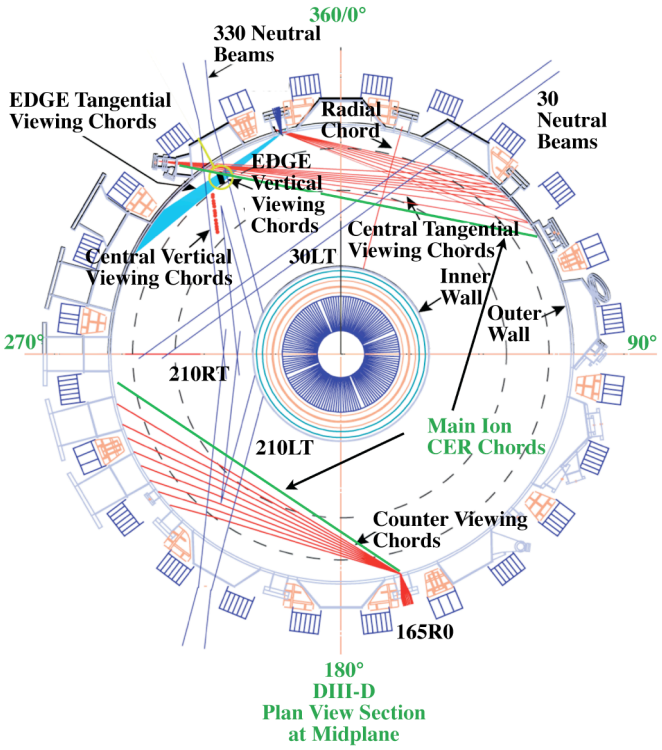

FIG. 1. Top-down view of the DIII-D tokamak showing the main ion diagnostic matched views of the 30° and 210° beams.

III. LIGHT EMISSION NEAR D_A

The spectral region near the deuterium (D_α) line at 6561.03Å for neutral deuterium beam injected plasmas contains bright emission from the cold plasma edge, emission due to charge exchange between beam neutrals and plasma ions, halo emission,[19] Stark-split beam neutral emission, D_α light from slowing down fast ions, and impurities [Fig. 2(a)]. The neutral halo which surrounds the injected beam is created by multiple charge exchange events between thermal ions and neutral deuterium born from direct charge exchange with the beam. The halo emits with the true ion temperature and rotation, but is spatially diffuse and limits the diagnostic spatial resolution. Modulation of the neutral beam injection and timeslice subtraction is used to eliminate the complicating features of edge emission and impurity lines in ELM-free discharges [Fig. 2(b)]. However, the formation of the halo, charge exchange with fast ions, as well as the beam emission itself are caused by neutral beam injection and cannot be eliminated with timeslice subtraction.

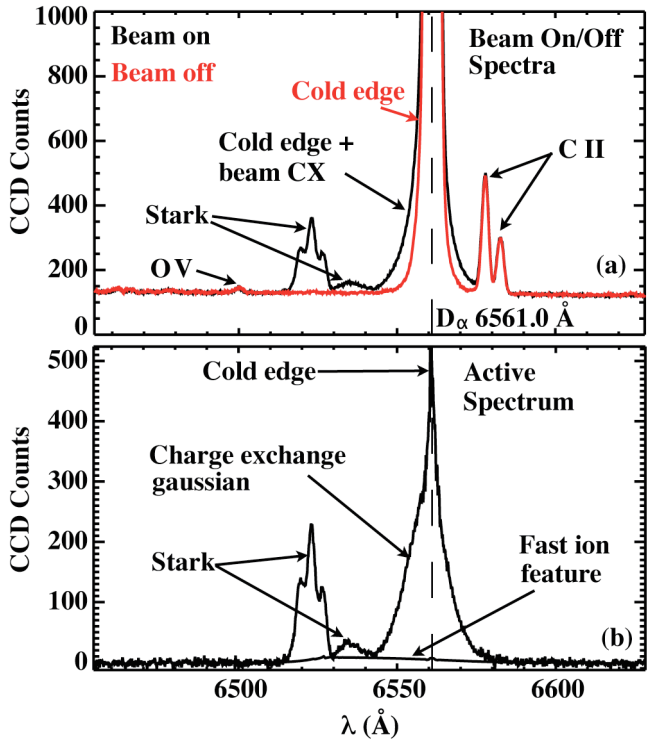

FIG. 2. (a) The spectral range of D_α includes cold emission near the plasma edge, beam emission and impurities. (b) Timeslice subtraction produces the active emission from beam injection and eliminates the impurity lines.

IV. CHARGE EXCHANGE CROSS SECTION

The direct charge exchange process between injected beam neutrals and plasma ions produces D_α light with an intensity

$$I \propto n_b n_i \sigma^{CX}(v_r) v_r \quad , \tag{1}$$

where n_b is the beam neutral density, n_i is the ion density, σ is the charge exchange cross section, and v_r is the relative velocity between injected beam neutrals and plasma ions $v_r = |\mathbf{v} - \mathbf{v}_b|$. The rate coefficient[20] is displayed in Fig. 3. The existence of molecular deuterium in the neutral beam ion source results in three beam species at energies $E = E_0$, $E_0/2$, $E_0/3$, and the rate coefficient must be summed for each beam energy component with respective fractions. The velocity $\mathbf{v}$ also includes the bulk plasma rotation, in addition to the thermal velocity spread. It is the non-zero temperature which is the source of the energy dependent charge exchange cross-section effect, which can result in an apparent velocity shift in a stationary plasma.[15] The rate coefficient of the charge exchange process is displayed in Fig. 3. For neutral beam voltage of 81 kV, the full energy beam component falls on the high energy side of the peak rate, whereas the half and third beam components on the low energy side of the peak. Physically, ions moving in the same direction as the beam injection have a higher likelihood of undergoing charge exchange with the full energy injected beam neutrals. These ions contribute more strongly to one side of the spectrum. The enhancement to the blue or red side of the spectrum depends on viewing angle with respect to the beam injection. The situation is opposite for charge exchange reaction with the other two beam components, which have a higher coefficient when moving towards the beam.

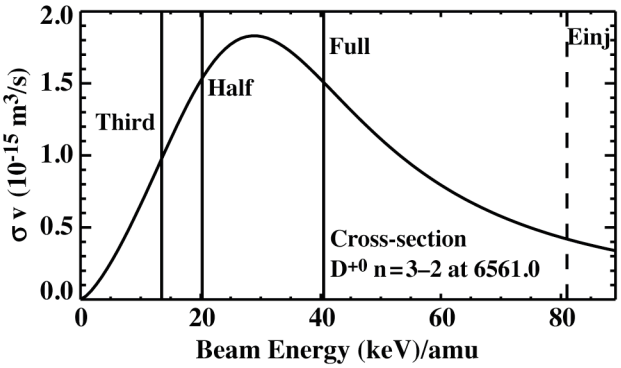

Fig. 3. The rate coefficient of the direct charge exchange process. The injector energy *Einj* is 81 kV. Full, half, and third energies for neutral deuterium injection are displayed (ADAS).

V. MAIN ION TEMPERATURE AND ROTATION MEASUREMENT IN FAVORABLE PLASMA CONDITIONS

In low temperature $T_i \lesssim 2$ keV and high density $n_e \approx 7\times10^{19}$ m^{-3} H-mode discharges, the conditions are favorable for main ion spectroscopy. Flat core profiles of temperature and rotation reduce the effects of spatial smearing due to spatial gradients and halo emission. The fast ion slowing down feature in the observed spectrum is minimized due to the short fast slowing down time and low beam power. The low ion temperature produces weak distortions to the thermal charge exchange line shape, which can be represented by a Gaussian. Utilizing the multi-Gaussian fitting routine, the spectra have been fit with a single Gaussian representing the thermal charge exchange with the beam and halo contribution (Fig. 4). The warm edge charge exchange emission at temperatures less than 0.1 keV, and electron impact excited cold edge neutral emission with temperatures less than 0.01 keV are both fit with Gaussian shapes with restricted temperature ranges. The Stark-split beam emission is fit with a complete Stark manifold.[21] The D_α contribution from fast ions slowing down is modeled by an analytic form,[22] and has a small amplitude in this discharge ($\approx$2% of the thermal charge exchange emission). The quality of the fit is displayed in the weighted residual in Fig. 4 which is at uniform noise amplitude across the entire D_α spectral range.

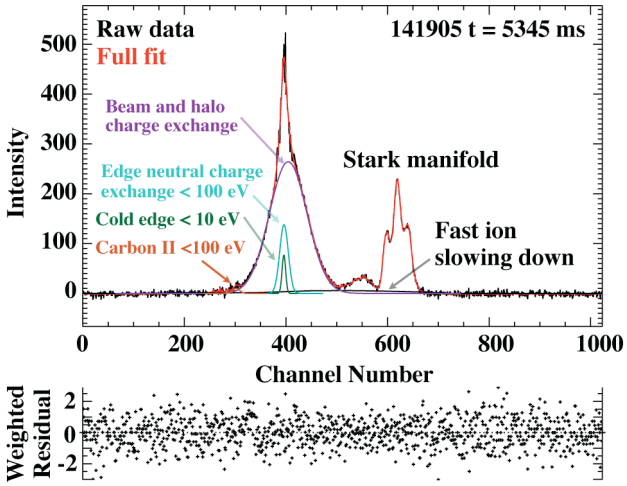

FIG. 4. Fit of the active D_α emission (model described in text) obtained at 2.5 ms integration time. The high accuracy of the fit model is demonstrated by the uniform low amplitude residual at the noise level.

The main ion results for four timeslices over a 10 ms beam pulse are displayed in Fig. 5, along with the impurity carbon profile. The temperature measurement [Fig. 5(a)] is in good agreement both between the two independent measurements of co (○) and counter (◊) views, as well as with the carbon profile. This is expected due the strong collisional coupling amongst ion species.

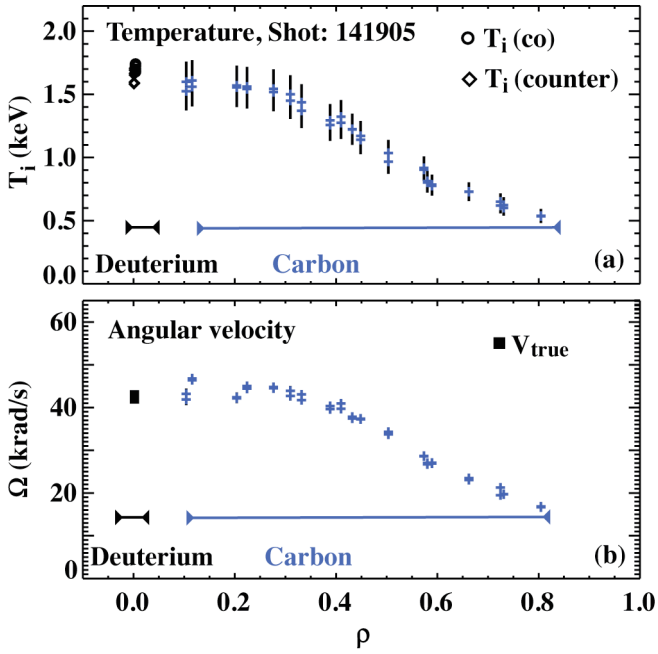

FIG. 5. Profiles of (a) ion temperature and (b) toroidal rotation frequency for both carbon and deuterium spectroscopic measurements. The temperature profile displays the apparent temperatures for each viewing chord. The rotation profile displays the true velocity $\mathbf{V}_{true}$ calculated by the method detailed in Ref. 14.

The apparent rotation values for the co view is $\Omega^D_{app,co} \approx 57$ krad/s. The apparent rotation for the counter view is $\Omega^D_{app,counter} \approx 36$ krad/s. The true deuterium toroidal rotation, which lies between the two apparent rotation values is $\Omega^D_{true} \approx 43$ krad/s calculated by the method detailed in Ref. 18. Each point from the four timeslices is overplotted in Fig. 5(b) (■). The main ion rotation is in reasonable agreement with the carbon measurement for these discharge parameters where the differential rotation is expected to be small. The atomic The close agreement between the deuterium and carbon rotation is due to the weak pressure gradient in this region of the plasma producing a small diamagnetic term in the radial force balance equation. The atomic correction to these rotation values using only the rate coefficient in Fig. 3 brings the apparent rotation measurements into closer agreement with the true rotation, but fall short by approximately 50%. The full explanation of the velocity correction based on atomic cross sections for each view is the subject of ongoing research efforts. The halo contribution to the spectrum in steep gradient regions is being investigated with a three-dimensional simulation which models the beam attenuation and neutral halo diffusion.[23] The fast ion contribution is being benchmarked against numerical simulations for high temperature and high beam power discharges.

VI. CONCLUSIONS

A two-chord prototype main ion CER diagnostic is operational on DIII-D for measuring the temperature and toroidal rotation of the main ion species in deuterium plasmas with deuterium beam injection. The co and counter view method of determining true the main ion rotation velocity will enable routine calculations of impurity and deuterium differential rotation in DIII-D discharges, and provide comparisons with neoclassical rotation predictions from theory and simulations.

REFERENCES

[1]R. Isler, Plasma Phys. Control. Fusion **36**, 171 (1994).

[2]M. von Hellermann, W. Mandl, H. Summers, and H. Weisen, Rev. Sci. Instrum. **61**, 3479 (1990).

[3]D. Thomas, G. McKee, K. Burrell, F. Levinton, E. Foley, and R. Fisher, Fusion Sci. Technol. **53**, 487 (2008).

[4]E. Busche, H. Euringer, and R. Jaspers, Plasma Phys. Control. Fusion **39**, 1327 (1997).

[5]W. Mandl, Technical Report JET-IR(92)05, JET (1992).

[6]J. Svensson, M. von Hellermann, and R. König, Plasma Phys. Control. Fusion **43**, 389 (2001).

[7]D. Testa, C. Giroud, A. Fasoli, K. Zastrow, and E. Team, Phys. Plasmas **9**, 243 (2002).

[8]L. Baylor, K. Burrell, R. Groebner, W. Houlberg, D. Ernst, M. Murakami, and M. Wade, Phys. Plasmas **11**, 3100 (2004).

[9]D. Ernst, M. Bell, R. Bell, C. Bush, Z. Chang, E. Fredrickson, L. Grisham, K. Hill, D. Jassby, and D. Mansfield, Phys. Plasmas **5**, 665 (1998).

[10]J. S. deGrassie, J. E. Rice, K. H. Burrell, R. J. Groebner, and W. M. Solomon, Phys. Plasmas **14**, 056115 (2007).

[11]H. Eubank, R. Goldston, V. Arunasalam, M. Bitter, K. Bol, D. Boyd, N. Bretz, J. Bussac, S. Cohen, and P. Colestock, Phys. Rev. Lett. **43**, 270 (1979).

[12]R. Budny, M. Bell, H. Biglari, M. Bitter, C. Bush, C. Cheng, E. Fredrickson, B. Grek, K. Hill, and H. Hsuan, Nucl. Fusion **32**, 429 (1992).

[13]R. Budny, Nucl. Fusion **34**, 1247 (1994).

[14]R. Howell, R. Fonck, R. Knize, and K. Jaehnig, Rev. Sci. Instrum. **59**, 1521 (1988).

[15]M. von Hellermann, P. Breger, J. Frieling, R. Konig, W. Mandl, A. Maas, and H. Summers, Plasma Phys. Control. Fusion **37**, 71 (1995).

[16]K. H. Burrell, P. Gohil, R. J. Groebner, D. H. Kaplan, J. I. Robinson, and W. M. Solomon, Rev. Sci. Instrum. **75**, 3455 (2004).

[17]P. Gohil, K. H. Burrell, R. J. Groebner, and R. Seraydarian, Rev. Sci. Instrum. **61**, 2949 (1990).

[18]W. M. Solomon, K. H. Burrell, R. Feder, A. Nagy, P. Gohil, and R. J. Groebner, Rev. Sci. Instrum. **79**, 10F531 (2008).

[19]J. Hogan, J. Nucl. Mater. **111**, 413 (1982).

[20]URL http://www.adas.ac.uk.

[21]N. A. Pablant, K. H. Burrell, R. J. Groebner, D. H. Kaplan, and C. T. Holcomb, Rev. Sci. Instrum. **79**, 10F517 (2008).

[22]M. G. von Hellermann, W. G. F. Core, J. Frieling, L. D. Horton, R. W. T. Konig, W. Mandl, and H. P. Summers, Plasma Phys. Control. Fusion **35**, 799 (1993).

[23]W. W. Heidbrink, K. H. Burrell, Y. Luo, N. A. Pablant, and E. Ruskov, Plasma Phys. Control. Fusion **46**, 1855 (2004).

ACKNOWLEDGMENT

This work was partially supported by the U.S. Department of Energy under DE-AC02-09CH11466, DE-FC02-04ER54698 and DE-FG02-07ER54917. The originating developer of ADAS is the JET Joint Undertaking.